Supplement of Geosci. Model Dev., 19, 8815–8838, 2026
https://doi.org/10.5194/gmd-19-8815-2026-supplement

Geoscientific Model Development
Open Access
EGU

Supplement of

Evaluation of the LandscapeDNDC model for drained peatland forest managements, LDNDC v1.35.2 (revision 11434)

Ahmed Hasan Shahriyer et al.

Correspondence to: Ahmed Hasan Shahriyer (ahmed.hasan.shahriyer@fmi.fi)

1 supplementary material

1.1 Individual soil parameters from sensitivity tests and NSE_{NEE} distribution

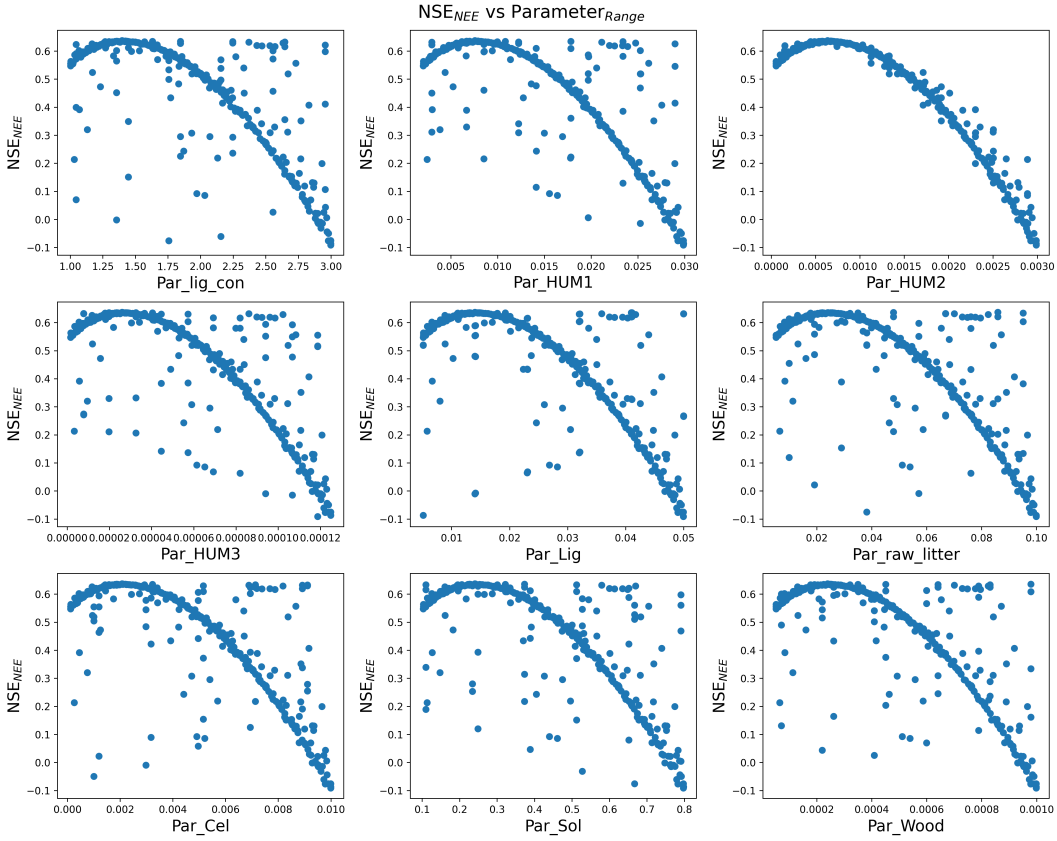

Figure S1. Distribution of Nash-Sutcliffe efficiency (NSE) values for net ecosystem exchange (NEE) from the sensitivity analysis of the first soil parameter set. Parameters in Sets 2 and 3 were fixed at their default values during the simulations.

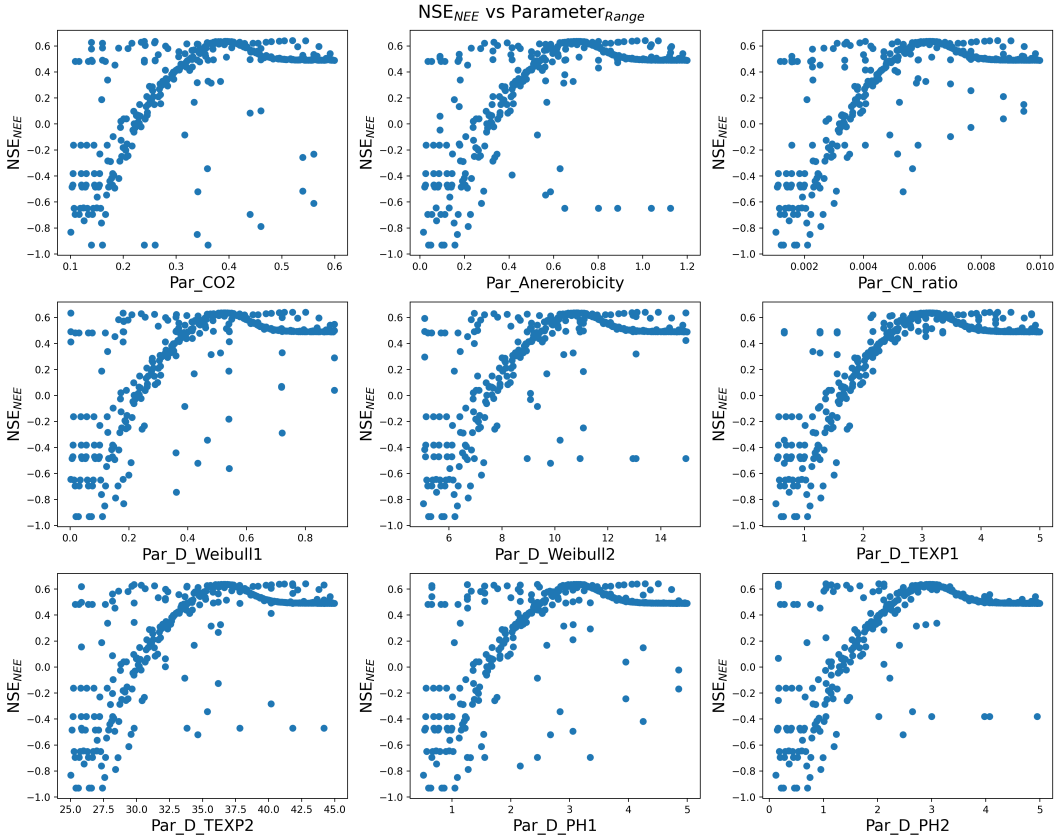

Figure S2. Distribution of Nash-Sutcliffe efficiency (NSE) values for net ecosystem exchange (NEE) from the sensitivity analysis of the second soil parameter set. Parameters in Set 1 were fixed to the values yielding the highest NSE extracted from first sensitivity test (Table A1), whereas parameters in Set 3 were maintained at their default values.

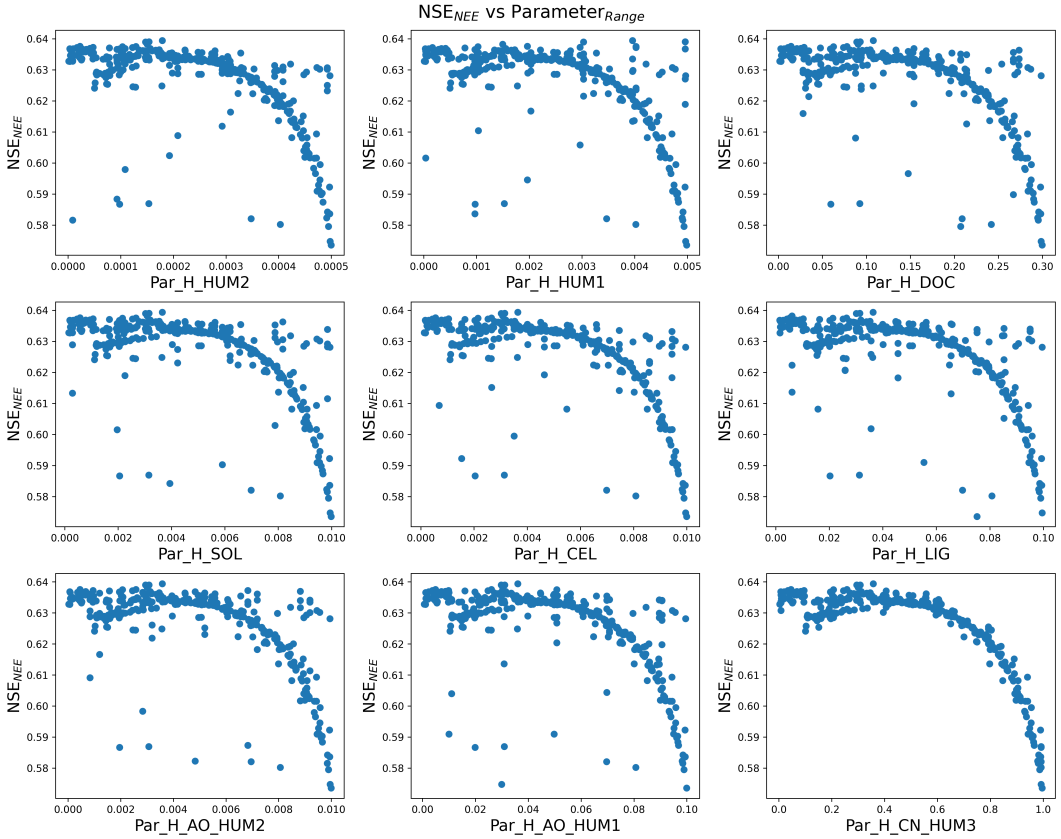

Figure S3. Distribution of Nash-Sutcliffe efficiency (NSE) values for net ecosystem exchange (NEE) from the sensitivity analysis of the third soil parameter set. Parameters in Sets 1 and 2 were fixed to the values yielding the highest NSE in the previous two analyses, respectively (Table A1).

1.2 Leaf area index

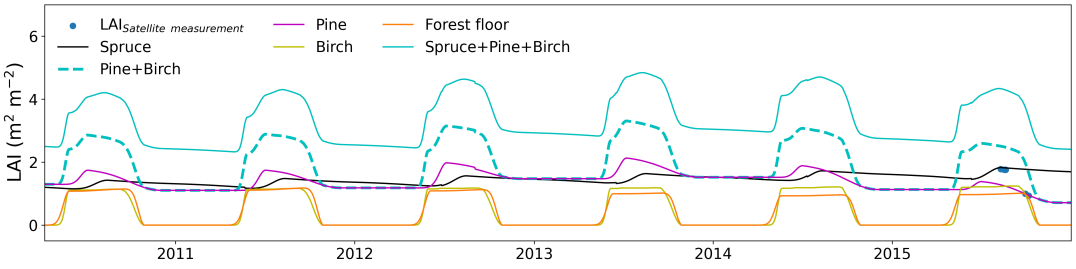

Figure S4. Simulated pre-harvest one-sided leaf area index (LAI) for individual tree species. The cyan solid line shows the total LAI of spruce, pine, and birch combined, whereas the cyan dashed line shows the combined LAI of pine and birch.

1.3 Water table

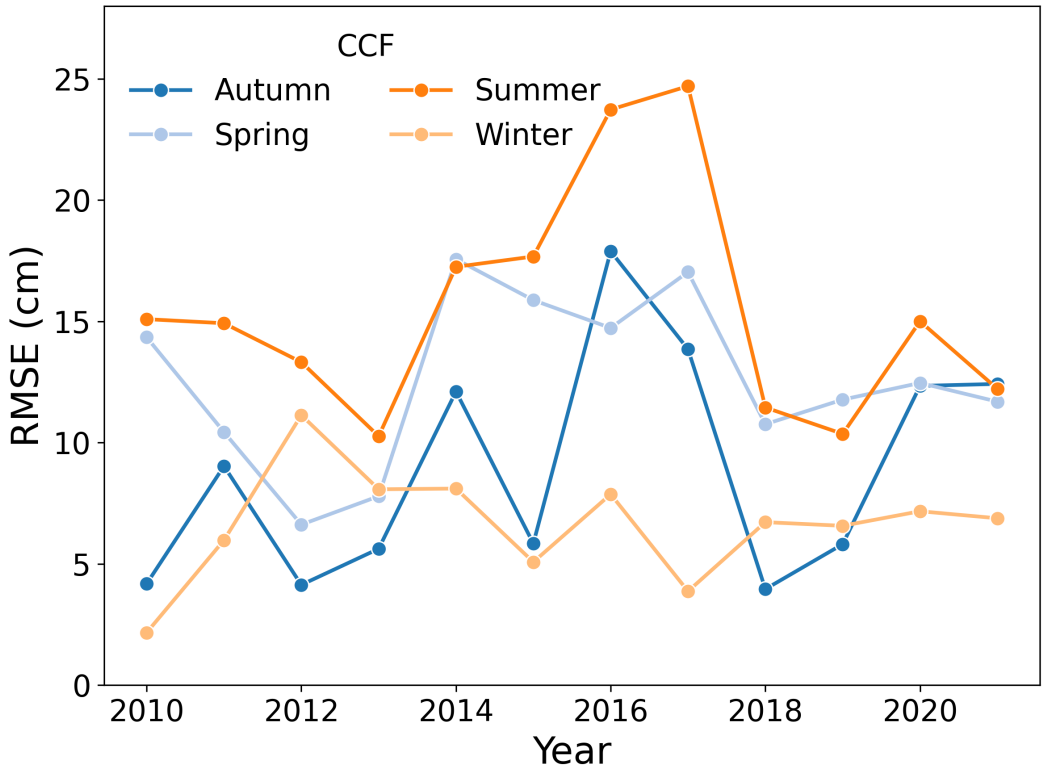

Figure S5. Seasonal root mean square error (RMSE) between simulated and observed water table (WT) levels at the continuous cover forestry stand.

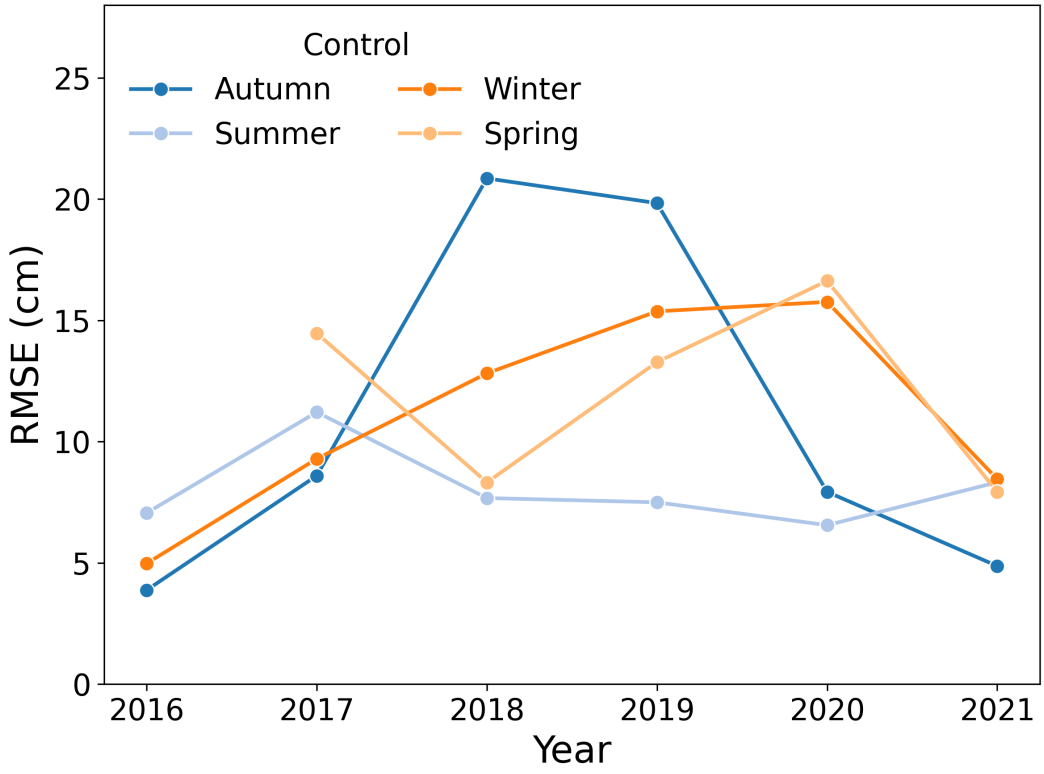

Figure S6. Seasonal root mean square error (RMSE) between simulated and observed water table (WT) levels at the control stand.

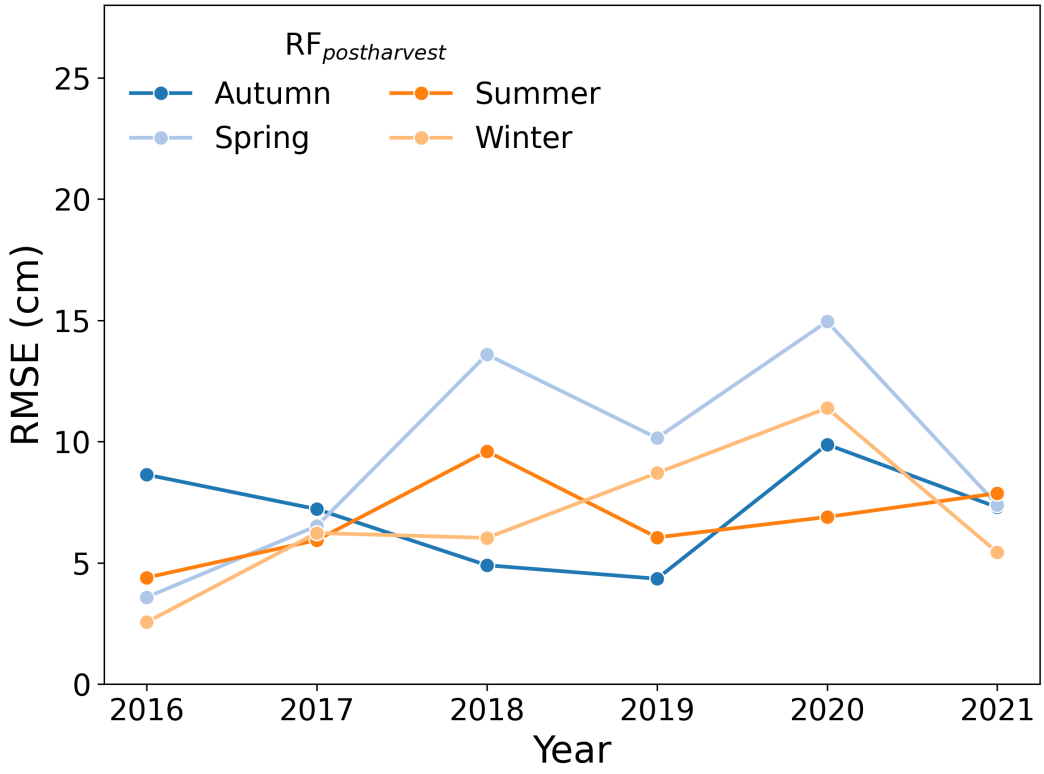

Figure S7. Seasonal root mean square error (RMSE) between simulated and observed water table (WT) levels at the rotational forestry stand.

1.4 Dynamics of CO_2 exchange before and after harvest

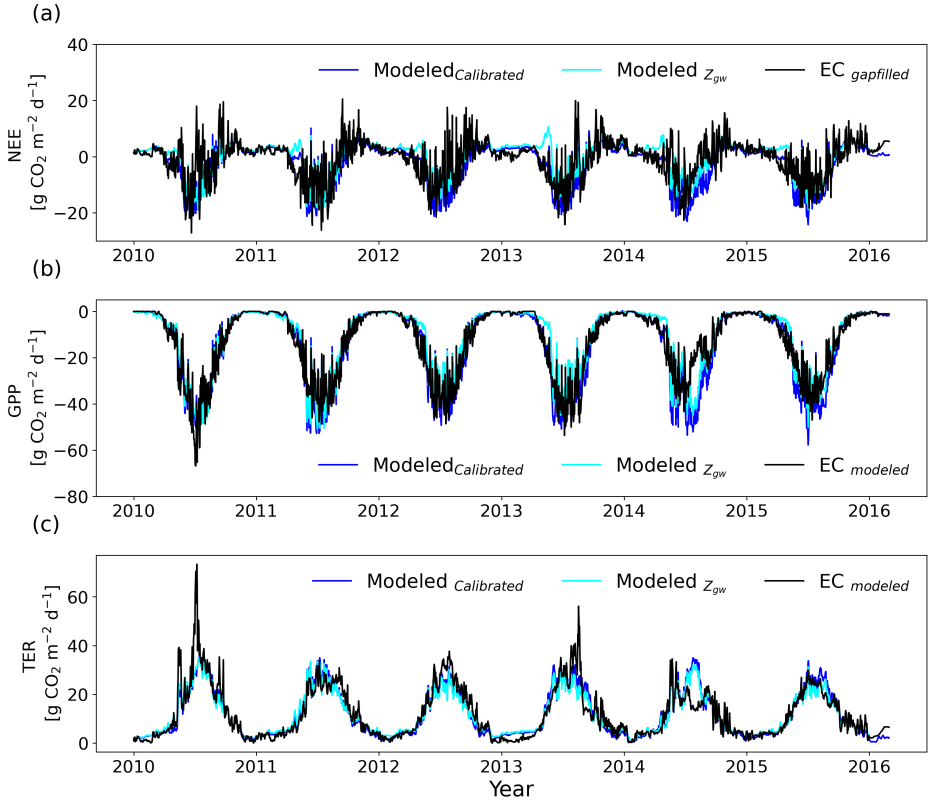

Figure S8. Daily sums of **(a)** NEE, **(b)** GPP and **(c)** TER under pre-harvest conditions in continuous cover forestry stand. Cyan and black lines indicate modeled CO_2 fluxes using the reference water table (Z_{gw}) and calibrated water table, respectively. EC-based estimates of CO_2 fluxes are shown in blue. Negative values denote ecosystem CO_2 uptake, and positive values denotes CO_2 emissions to the atmosphere.

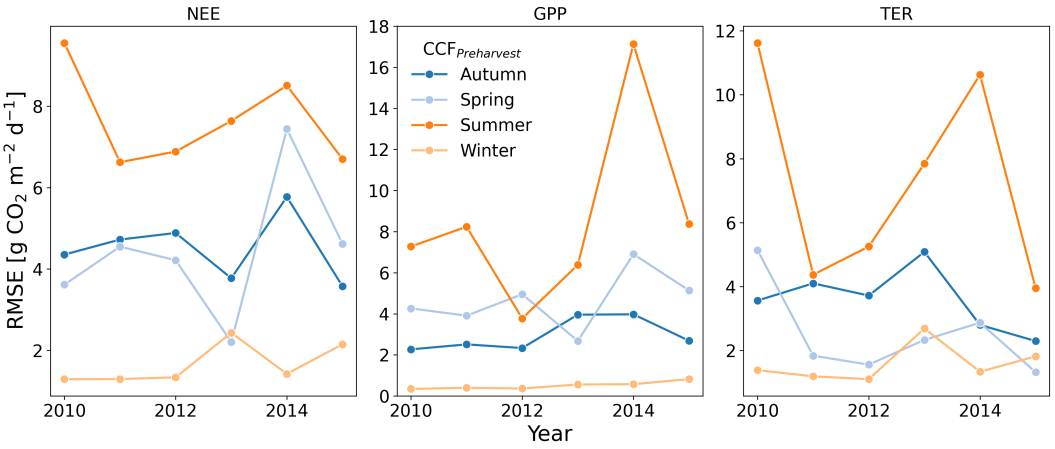

Figure S9. Seasonal Root Mean Square Error (RMSE) of NEE between Model and observations under pre-harvest conditions in continuous cover forestry stand.

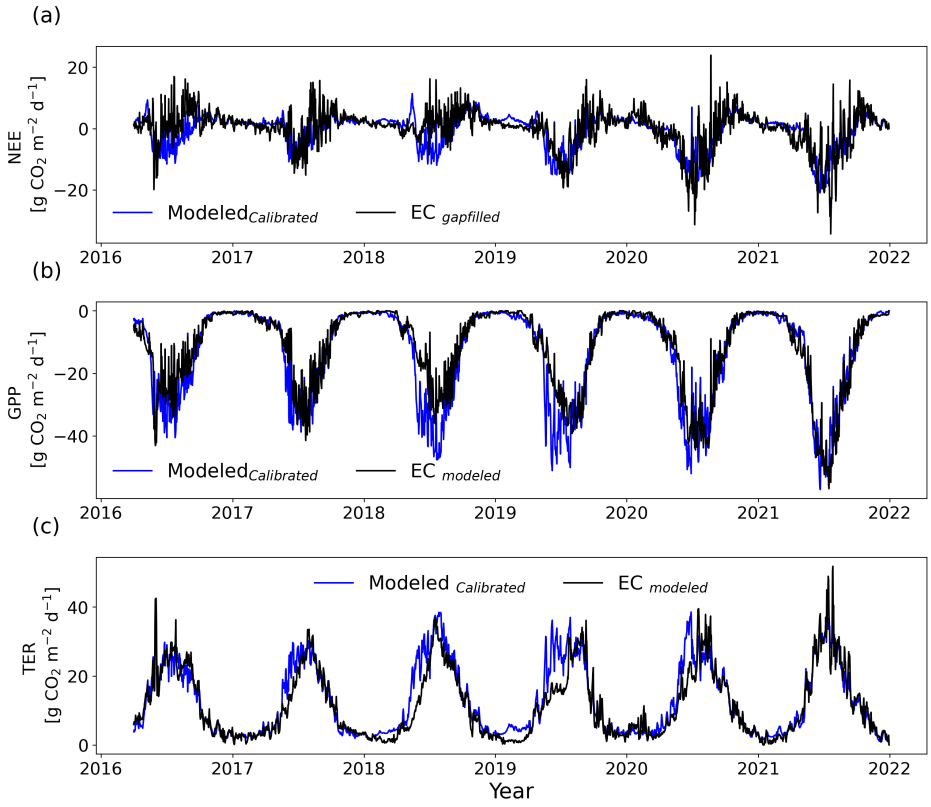

Figure S10. Daily sums of **(a)** NEE , **(b)** GPP and **(c)** TER under post-harvest conditions in continuous cover forestry stand. Blue and black lines indicate the modeled and EC-based estimates, respectively. Negative values denote ecosystem CO_2 uptake, and positive values denotes CO_2 emissions to the atmosphere.

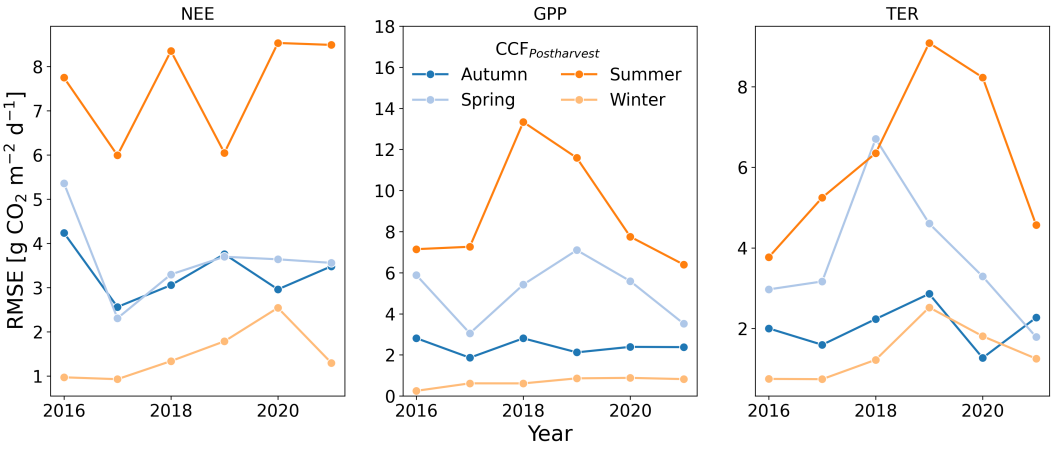

Figure S11. Seasonal Root Mean Square Error (RMSE) of NEE between model and observations under post-harvest conditions in continuous cover forestry stand.

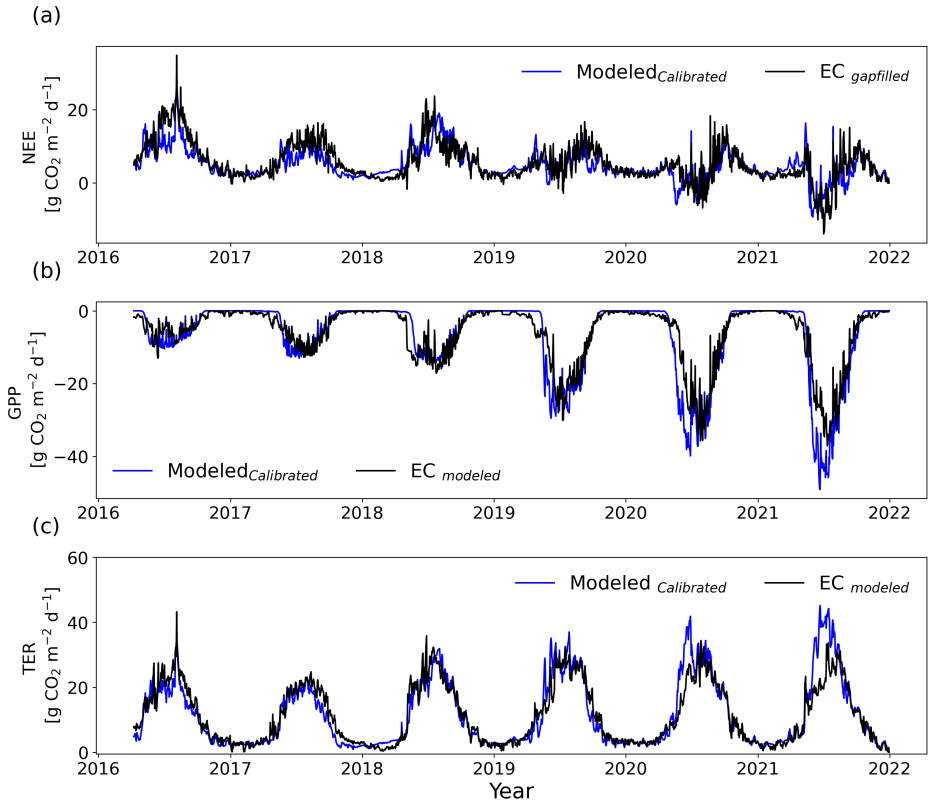

Figure S12. Daily sums of **(a)** NEE, **(b)** GPP and **(c)** TER under post-harvest conditions in rotational forestry stand. Blue and black lines indicate the modeled and EC-based estimates, respectively. Negative values indicate uptake by the ecosystem, and positive values indicate the emission of CO_2 into the atmosphere.

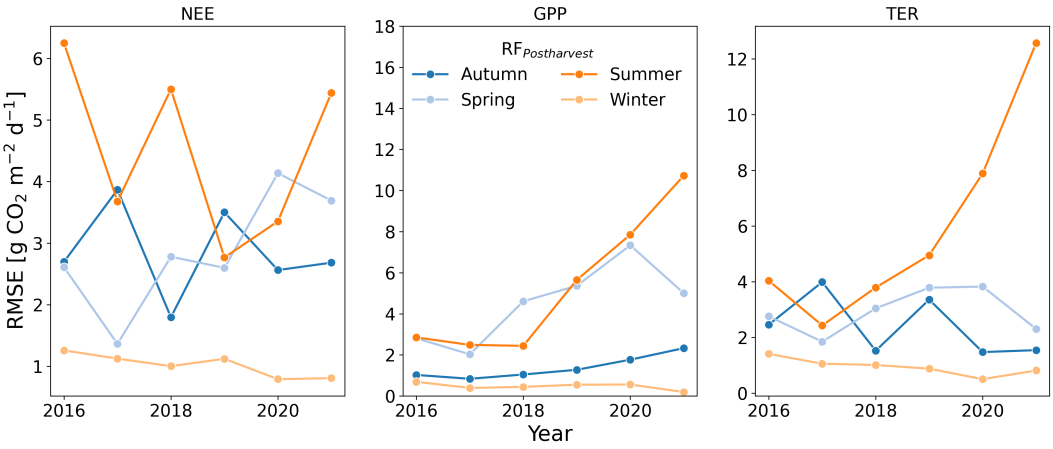

Figure S13. Seasonal Root Mean Square Error (RMSE) of NEE between Model and observations under post-harvest conditions at rotational forestry stand.

Using half-hourly data, model performance for NEE was highest during the pre-harvest period (r = 0.82, NSE = 0.66), followed by RF$_{postharvest}$ (r = 0.79, NSE = 0.57) and CCF$_{postharvest}$ (r = 0.72, NSE = 0.49) (Fig. S14a-c). For GPP, correlation coefficients ranged from 0.93 to 0.94 and NSE values from 0.69 to 0.84 (Fig. S14d-f). TER was also reproduced well, with r values between 0.88 and 0.92 and NSE values between 0.75 and 0.81 (Fig. S14g-i).

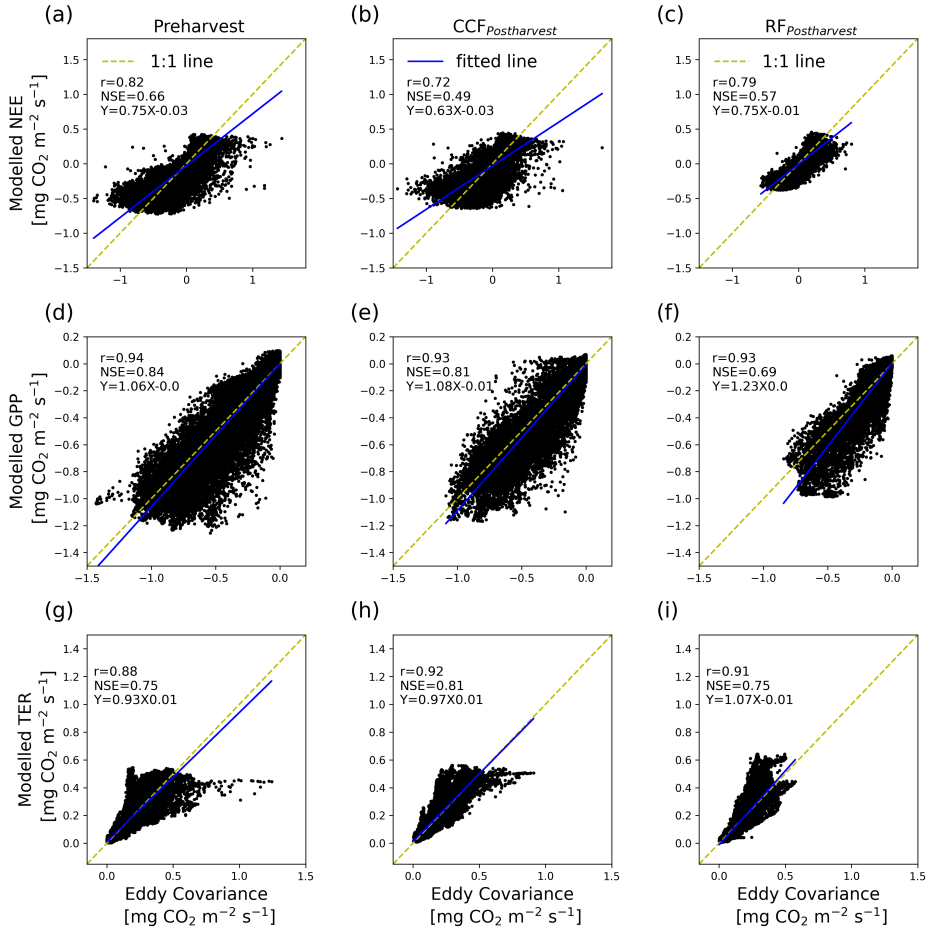

Figure S14. Half-hourly comparisons between modeled and observed NEE (a-c), GPP (d-f) and TER (g-i) under pre-harvest, CCF$_{postharvest}$ and RF$_{postharvest}$ conditions. Correlation coefficients (r) and Nash-Sutcliffe efficiency (NSE) values are provided in each panel. Yellow dashed lines indicate the 1:1 relationship, while blue lines represent the fitted regressions. The corresponding regression equations are given as Y.

1.5 Humus pool allocations

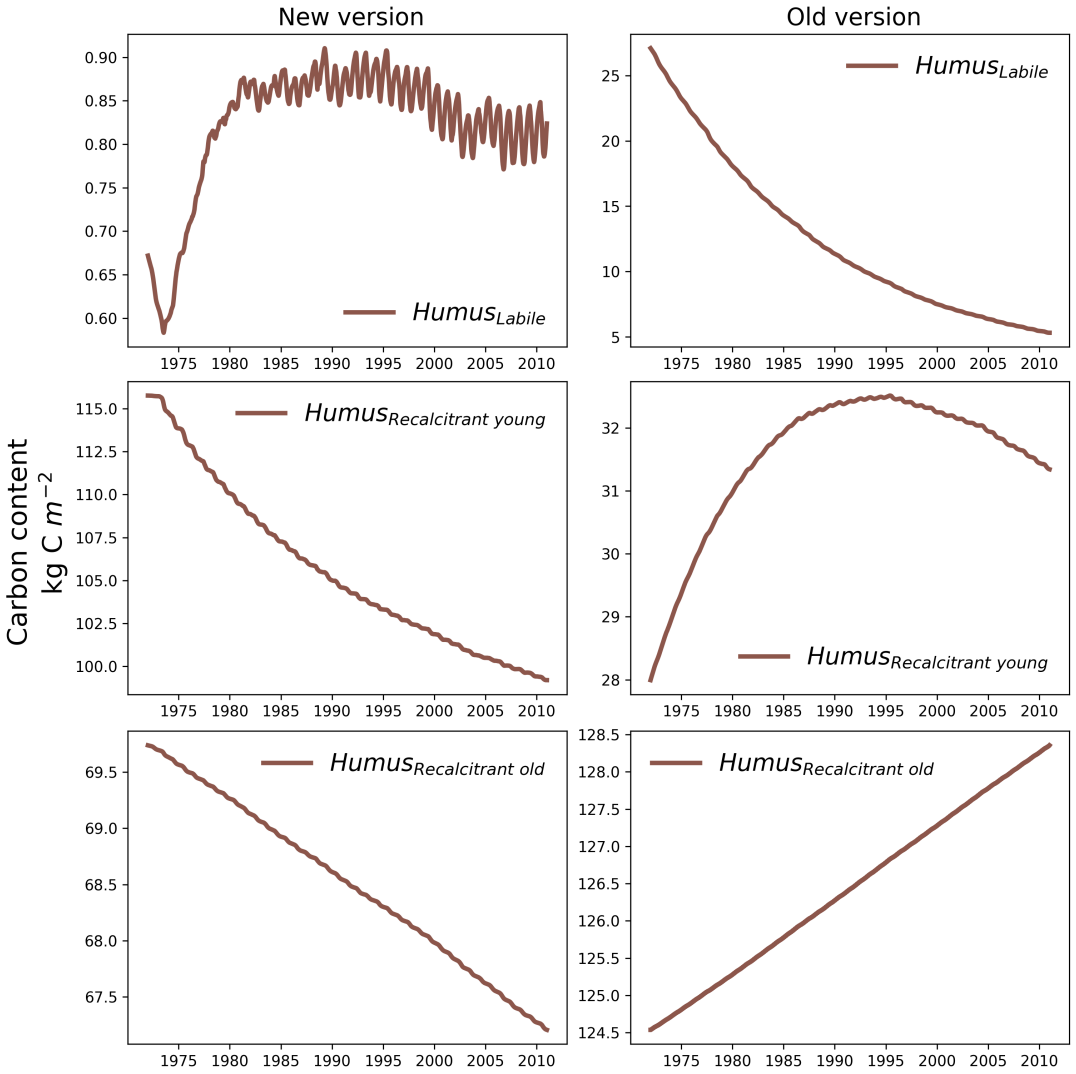

Figure S15. Carbon allocation among the different humus pools in the old and new model versions. In the new model version, the largest fraction of carbon was allocated to the recalcitrant young pool, whereas in the old model version the largest fraction was allocated to the recalcitrant old pool.

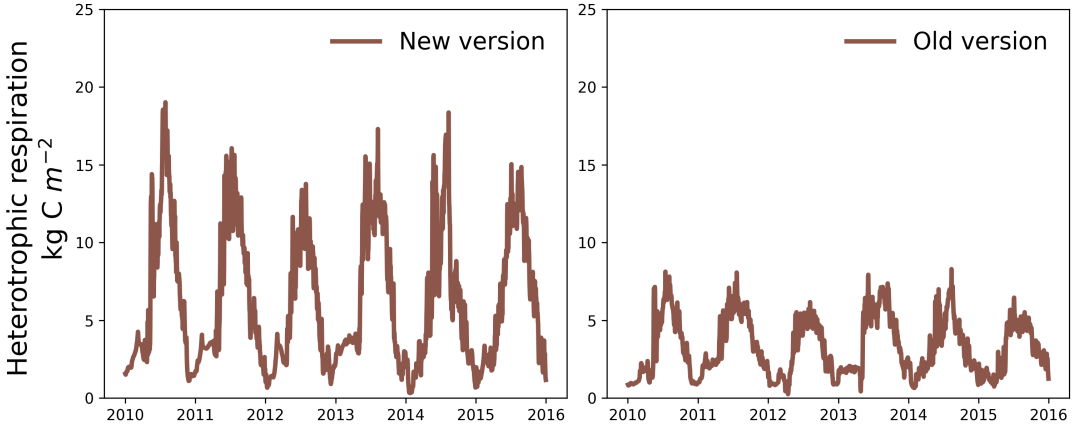

Figure S16. The new peat model version produced substantially higher heterotrophic respiration than the original mineral-soil version, reflecting the impact of the revised allocation of carbon among humus pools.